Supporting Information for "Insights on Continental Collisional Processes from GPS Data: Dynamics of the Peri-Adriatic Belts"

M. Métois[1], N. D'Agostino[1], A. Avallone[1] N. Chamot-Rooke[2], A. Rabaute[3],

L. Duni[4] N. Kuka[4], R. Koci[4] I. Georgiev[5]

Contents of this file

1. Text S1
2. Figures S1 to S12
3. Tables S1 to S6

Additional Supporting Information (Files uploaded separately)

1. Captions for large Tables S1 to S3

Introduction

This material presents informations relative to the data sources (Tables S1 and S2), the time-series length (Figure S3), the Eurasia-fixed reference frame realization (Figures S1 and S2) and the Euler poles estimated to rotate independant data sets in our reference

---

Corresponding author: M. Métois, Centro Nazionale Terremotti, Istituto Nazionale di Geofisica e Vulcanologia, via di Vigna Murata, 00145, Rome, Italy. (marianne.metois@ingv.it)

[1]Istituto Nazionale di Geofisica e

frame (Table 1). Details of the velocity field used in our study are given in the large Tables 1 to 3.

Figures S4 to S7 present the grid used for strain-rate calculation and alternative models conducted with different constrains.

Figures S8 to S9 show our velocity field together with other observations (anisotropy, rigid rotations).

Figure S10 is an Airy-isostasy test based on *Molinari and Morelli* [2011]'s crustal model. Figure 11 presents the theoretical GPE* generated by a interseismically locked crustal

Vulcanologia, Centro Nazionale Terremoti,
Via di Vigna Murata, 605, Roma, Italia

[2]Laboratoire de Gologie, Ecole Normale Suprieure, 24 rue Lhomond, 75005 Paris, France / CNRS UMR 8538

[3]GEOSUBSIGHT - ISTeP - UMR 7193 UPMC-CNRS, Universit Pierre et Marie Curie, 4 Place Jussieu, 75252 PARIS Cedex 05

[4]Institute of Geosciences, Tirana, Albania

[5]National Institute of Geophysics, Geodesy and Geography, Sofia, Bulgaria

fault. Figure 12 is equivalent to Figure 8 of the main text but considering a newtonian rheology for the lithosphere.

Text S1.

Here, we adapt the reasoning developed in section 4. of the main text to a lithosphere behaving as a Newtonian fluid. Therefore,

$$\tau_{ij} = 2\eta\dot{\epsilon}_{ij} \quad (1)$$

where τ_{ij} and and $\dot{\epsilon}_{ij}$ are the ij^{th} component of the deviatoric stress tensor averaged on the entire column of lithosphere and of the strain rate tensor, respectively, and η is the lithosphere viscosity.

Equations 5 and 6 can be expressed as

$$\partial_x\epsilon_{xx} + \partial_y\epsilon_{xy} - \partial_x\epsilon_{zz} = \frac{\partial_x\Gamma}{2\eta L} \quad (2)$$

$$\partial_y\epsilon_{yy} + \partial_x\epsilon_{xy} - \partial_y\epsilon_{zz} = \frac{\partial_y\Gamma}{2\eta L} \quad (3)$$

that implies $\Gamma^* = \Gamma/2\eta L$, where Γ^* is the dimensionless GPE calculated from the strain rate tensor, and Γ is the GPE derived from topography through equation 3 of the main text. In Figure S12, we plot the GPE* contours together with the GPE* gradients $\partial_x\Gamma^*$ and $\partial_y\Gamma^*$ and the filtered ETOPO1 topography.

Large table S1. Coordinates, horizontal components of the velocity, associated errors and correlation coefficient are presented for each GPS station processed in the Balkan-Eastern Alps area. Station name, duration of the time-serie in years, and bounding dates are indicated in columns 8 to 10. * - stations used for reference frame realization; **-core stations.

Large table S2. Coordinates, horizontal components of the velocity, associated errors and correlation coefficient are presented for each GPS station processed **in the broad Eastern Mediterranean area**. Station name, duration of the time-serie in years, and bounding dates are indicated in columns 8 to 10. * - stations used for reference frame realization; **- core stations.

Large table S3. Coordinates, horizontal components of the velocity, associated errors and correlation coefficient are presented for each GPS station processed and used for reference frame realization **out of or study zone**. Station name, duration of the time-serie in years, and bounding dates are indicated in columns 8 to 10. **- core stations.

References

Bertiger, W., S. D. Desai, B. Haines, N. Harvey, A. W. Moore, S. Owen, and J. P. Weiss (2010), Single receiver phase ambiguity resolution with gps data, *Journal of Geodesy*, *84*(5), 327–337.

Haines, A., and W. Holt (1993), A procedure for obtaining the complete horizontal motions within zones of distributed deformation from the inversion of strain rate data, *Journal of Geophysical Research: Solid Earth (1978–2012)*, *98*(B7), 12,057–12,082.

Jouanne, F., J. Mugnier, R. Koci, S. Bushati, K. Matev, N. Kuka, I. Shinko, S. Kociu, and L. Duni (2012), Gps constraints on current tectonics of albania, *Tectonophysics*, *554*, 50–62.

Kissel, C., F. Speranza, and V. Milicevic (1995), Paleomagnetism of external southern and central dinarides and northern albanides: Implications for the cenozoic activity of the scutari-pec transverse zone, *Journal of Geophysical Research: Solid Earth (1978–2012)*, *100*(B8), 14,999–15,007.

Kreemer, C. (2009), Absolute plate motions constrained by shear wave splitting orientations with implications for hot spot motions and mantle flow, *Journal of Geophysical Research: Solid Earth (1978–2012)*, *114*(B10).

Matev, K. (2011), Contraintes gps sur la tectonique actuelle du sud-ouest de la bulgarie, de la grèce du nord et de l'albanie, Ph.D. thesis, Université de Grenoble.

McCaffrey, R. (2005), Block kinematics of the pacific–north america plate boundary in the southwestern united states from inversion of gps, seismological, and geologic data, *Journal of Geophysical Research: Solid Earth (1978–2012)*, *110*(B7).

Molinari, I., and A. Morelli (2011), Epcrust: a reference crustal model for the european plate, *Geophysical Journal International*, *185*(1), 352–364.

Nocquet, J.-M. (2012), Present-day kinematics of the mediterranean: A comprehensive overview of gps results, *Tectonophysics*, *579*, 220–242.

Perouse, E., N. Chamot-Rooke, A. Rabaute, P. Briole, F. Jouanne, I. Georgiev, and D. Dimitrov (2012), Bridging onshore and offshore present-day kinematics of central and eastern mediterranean: Implications for crustal dynamics and mantle flow, *Geochemistry, Geophysics, Geosystems*, *13*(9).

Pondrelli, S., S. Salimbeni, G. Ekström, A. Morelli, P. Gasperini, and G. Vannucci (2006), The italian cmt dataset from 1977 to the present, *Physics of the Earth and Planetary Interiors*, *159*(3), 286–303.

Pondrelli, S., S. Salimbeni, A. Morelli, G. Ekström, L. Postpischl, G. Vannucci, and E. Boschi (2011), European–mediterranean regional centroid moment tensor catalog: solutions for 2005–2008, *Physics of the Earth and Planetary Interiors*, *185*(3), 74–81.

Wüstefeld, A., G. Bokelmann, G. Barruol, and J.-P. Montagner (2009), Identifying global seismic anisotropy patterns by correlating shear-wave splitting and surface-wave data, *Physics of the Earth and Planetary Interiors*, *176*(3), 198–212.

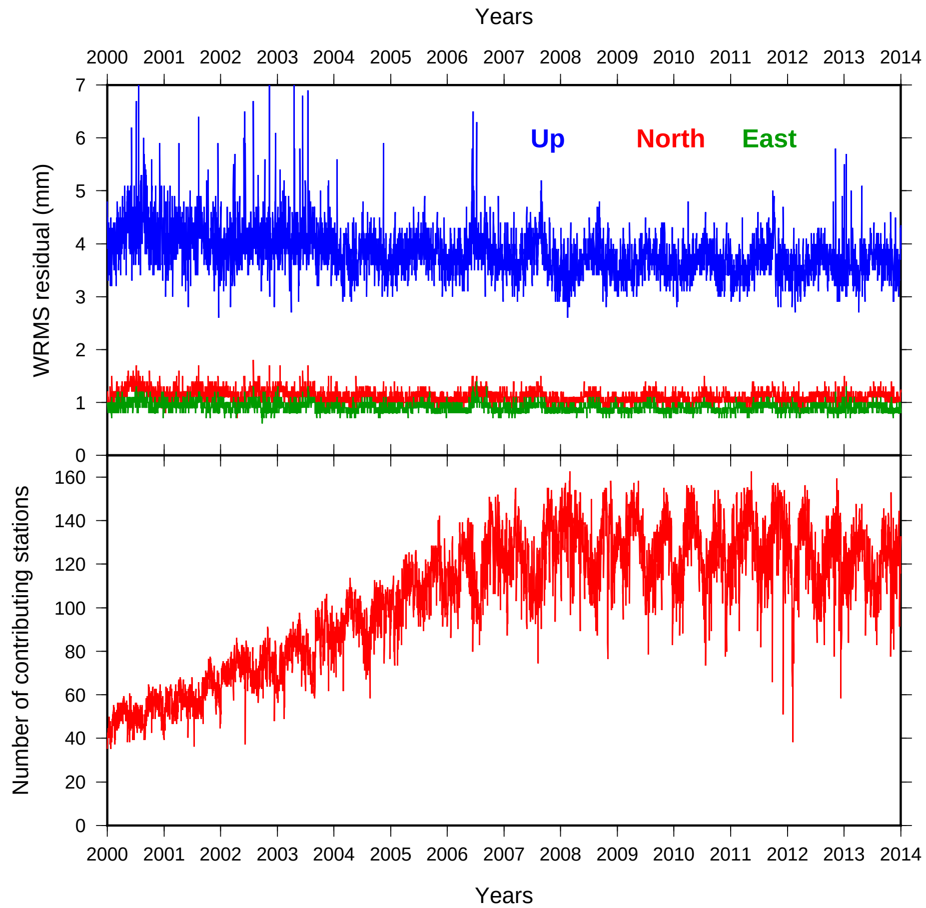

Figure S1. **Repeatabilities and stations involved in our Eurasian-fixed reference frame** - WRMS of the difference between predicted and observed coordinates (upper panel) and number (lower panel) of stations participating in our new reference frame.

Data set	Original reference frame	Rotation pole	Stations used	<res E>	<res N>
[*Jouanne et al.*, 2012]	ITRF2005	-46.04°E 69.35°N -0.245°/Myr	AMUR-CRLM-CCRI MATE-SRJV-LUZZ-SERS	0.33	0.4
[*Nocquet*, 2012]	fixed eurasia	46.92°E 23.13°N -0.039°/Myr	COST-BERA-SHKO DUBR-OSJE	0.50	0.6
[*Matev*, 2011]	fixed eurasia from ITRF2005	no rotation	no common points or too large uncertainties *Perouse et al.* [2012]	-	-

Table S1. Rotations applied when possible to previously published data sets to be combined with our own solution in our Eurasia-fixed reference frame.

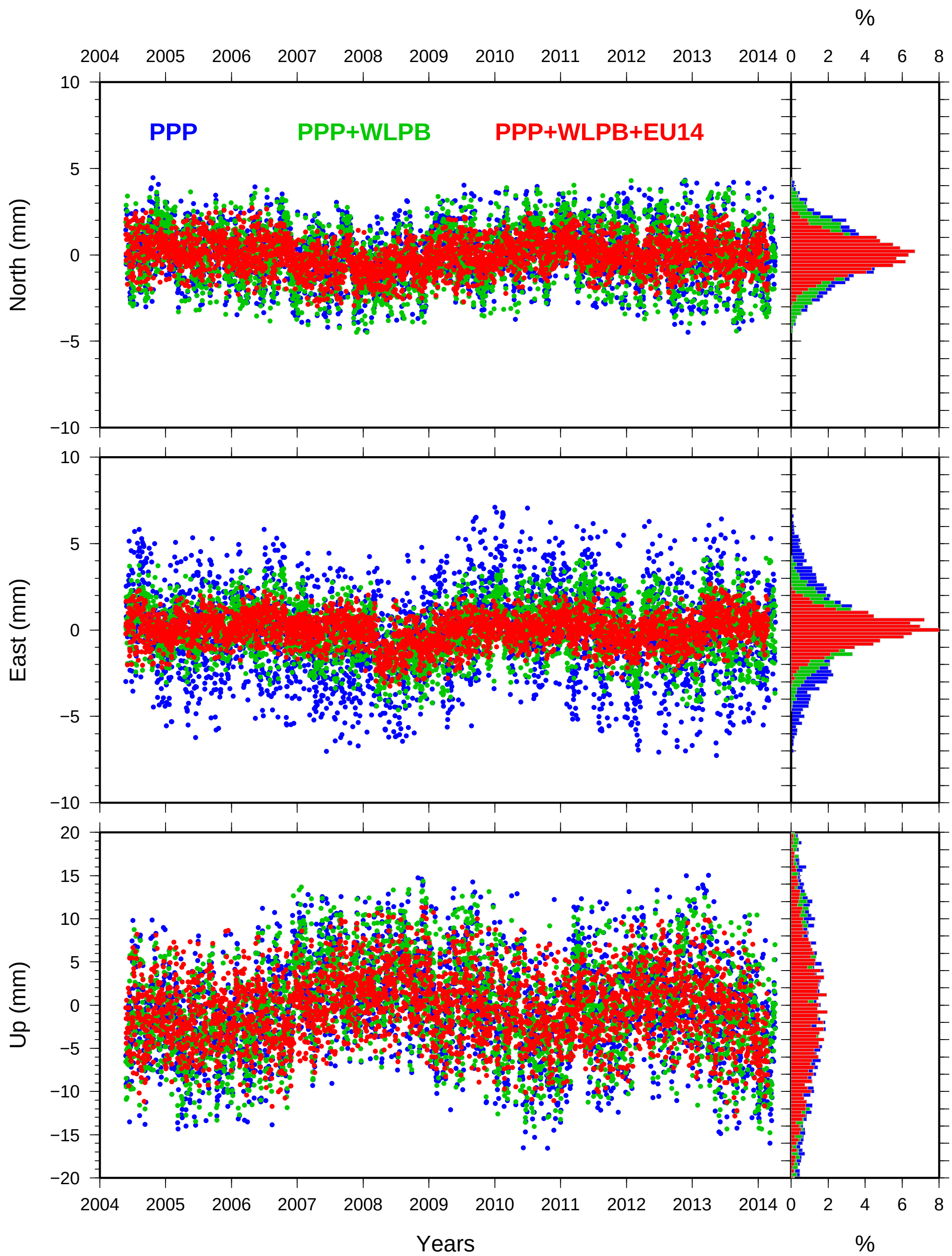

Figure S2. **Effect of processing strategies on time-series** - Example of the time series of GROT (detrended) and effects of different strategies on time series accuracy. Progressively reduced daily scatter is obtained, especially for the East component, by applying the WLPB strategy *Bertiger et al.* [2010] and our new reference frame alignment.

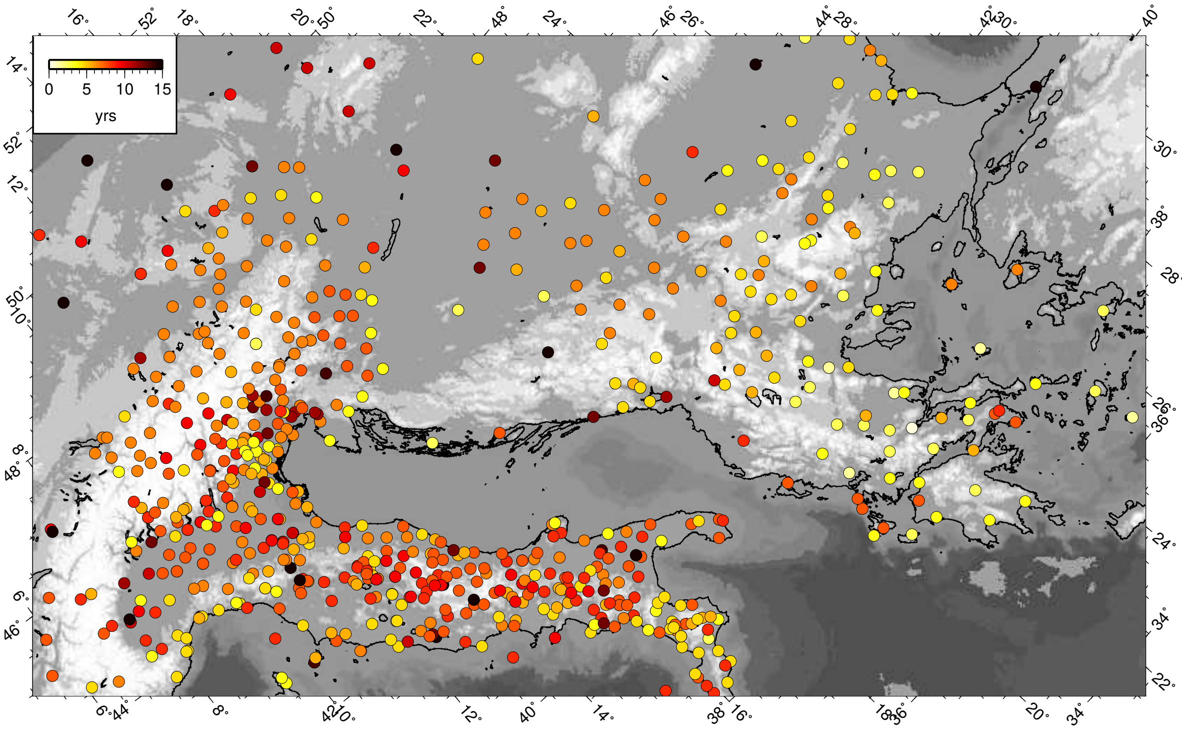

Figure S3. Map showing the length of the time-series used to calculate interseismic velocity for each station of our study area.

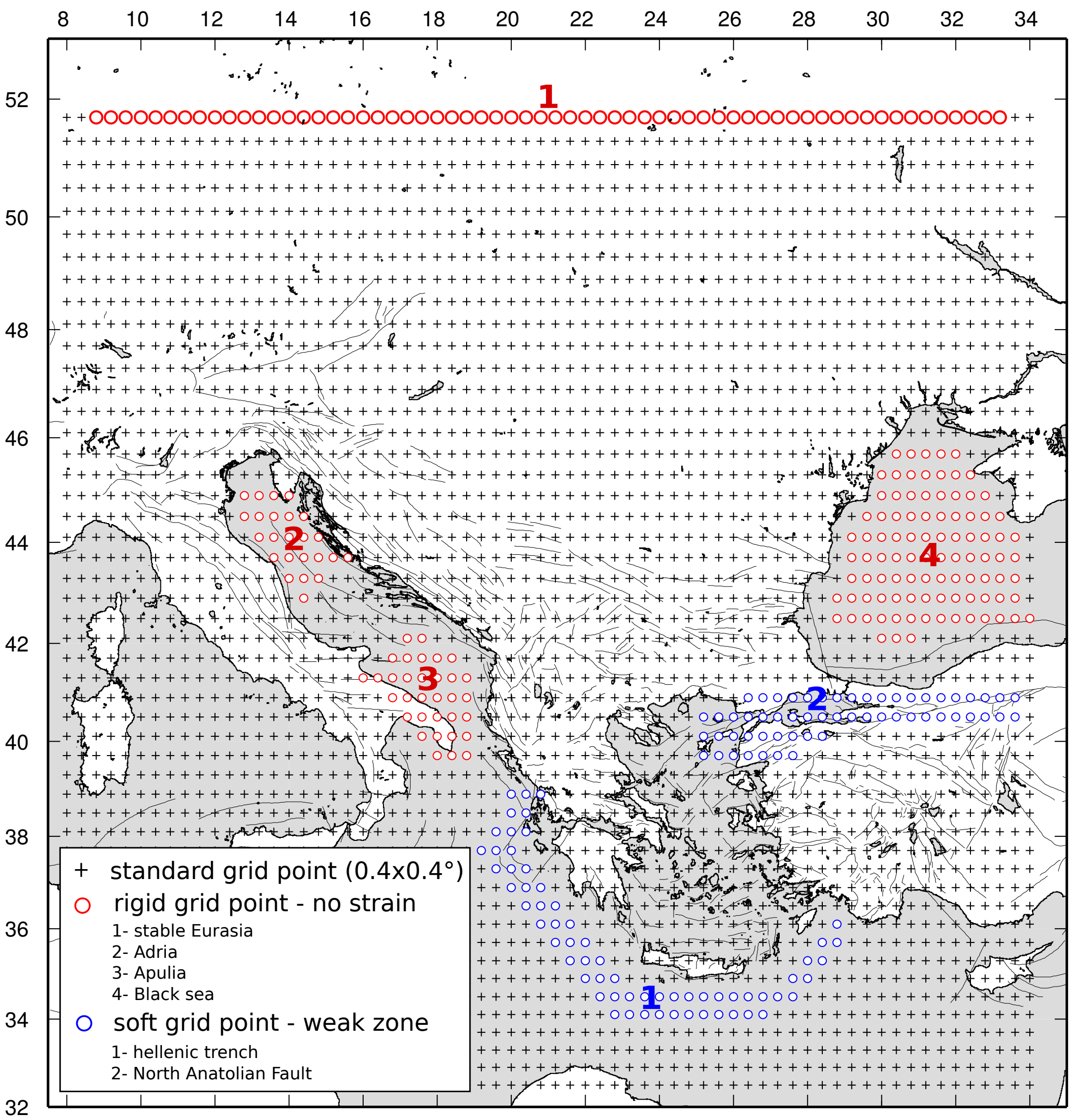

Figure S4. Grid used for strain calculation-Geometry of the 0.4°x0.4° grid built for strain calculation using the SPARSE program [*Haines and Holt*, 1993]. Circles : nodes fixed to be rigid or highly deforming (blue) depending on the model used. In our best model presented in the main text (Figures 3 to 5), the North Anatolian fault and Hellenic Backstop (1-2) are allowed to strain at high rates and the northernmost nodes raw is fixed to be rigid (1). Strain calculation forcing Adria, Apulia and Black Sea to be rigid is presented in Fig.S7 but this model does not produce any significant changes in the strain rate tensor nor the interpolated velocity field.

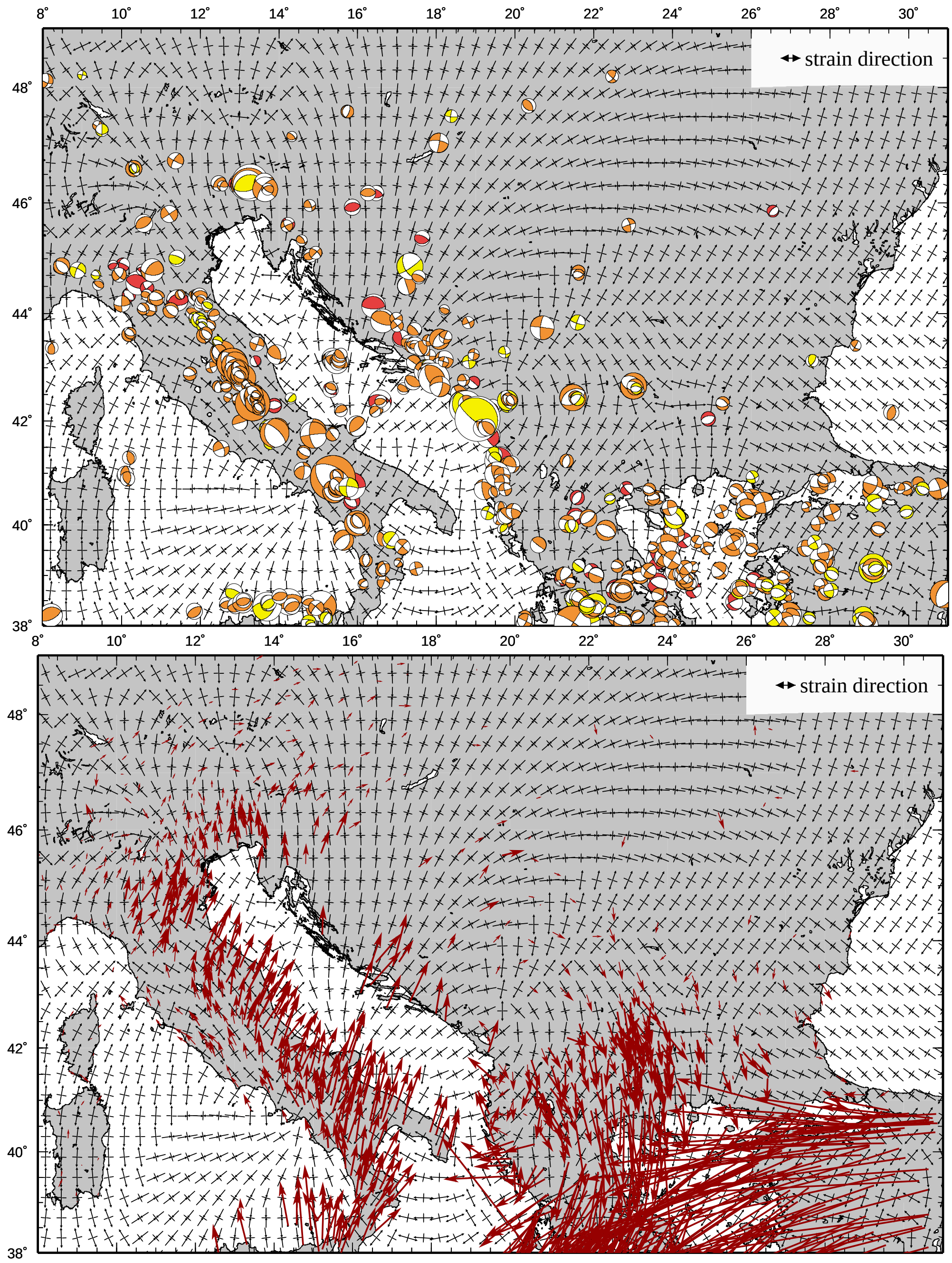

Figure S5. Strain axes derived from the RCMT and CMT catalogs- Here we use RCMT and CMT [*Pondrelli et al.*, 2006, 2011] focal mechanisms on the 1977-2011 period to derive the principal component of the strain rate tensor. We use the direction of the principal strain from this homogeneous field, disregarding its amplitude, as a constrain in the best model presented in the main text. Since very few mechanisms area available in the Balkans, using this information derived from the earthquake catalogs does not significantly modify the strain rate distribution nor the interpolated velocity field. It is to note that based on the focal mechanisms only, we reproduce part of the rotation pattern observed in the GPS data (bottom).

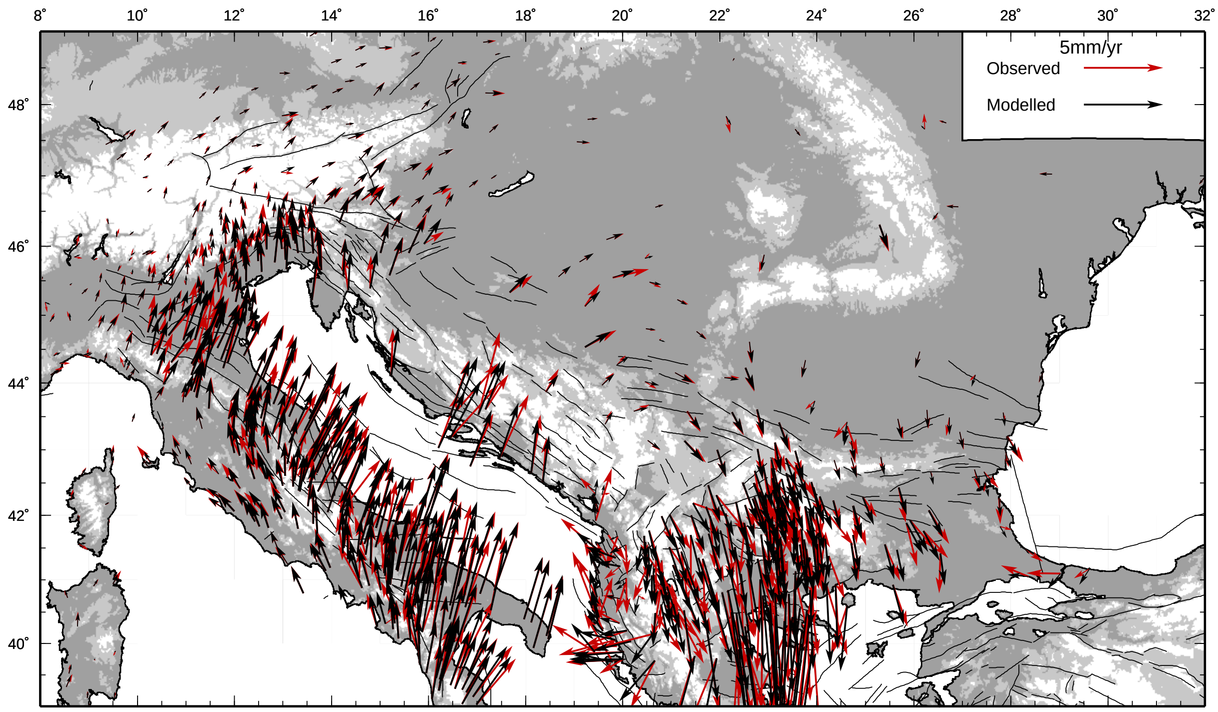

Figure S6. Predicted (black) and observed (red) velocities in our study area for our best model presented in the main text (Figure 3 to 5). Normalized root mean square in the Balkan area is 1.26.

Network	Description	Website
AGROS	Serbian Republic Geodetic Authority	www.rgz.gov.rs/agros
ALBANIA	GPSscope stations in Albania	https://gpscope.dt.insu.cnrs.fr
APOS	Austrian GPS permanent network	www.bev.gv.at
BULGARIA	Bulgarian network	www.hemus-net.org
		www.niggg.bas.bg
		www.naviteq.net
NOA	National Observatory of Athens	www.gein.noa.gr
MAKPOS	Macedonia network	www.makpos.katastar.gov.mk
METRICA	Greek network	www.metricanet.gr
SIGNAL	Slovenia National Network	www.gu-signal.si
TGREF	Private Bulgarian network	www.topgeocart.ro

Table S2. Description and address of the Networks processed for the Balkan-Eastern Alps area.

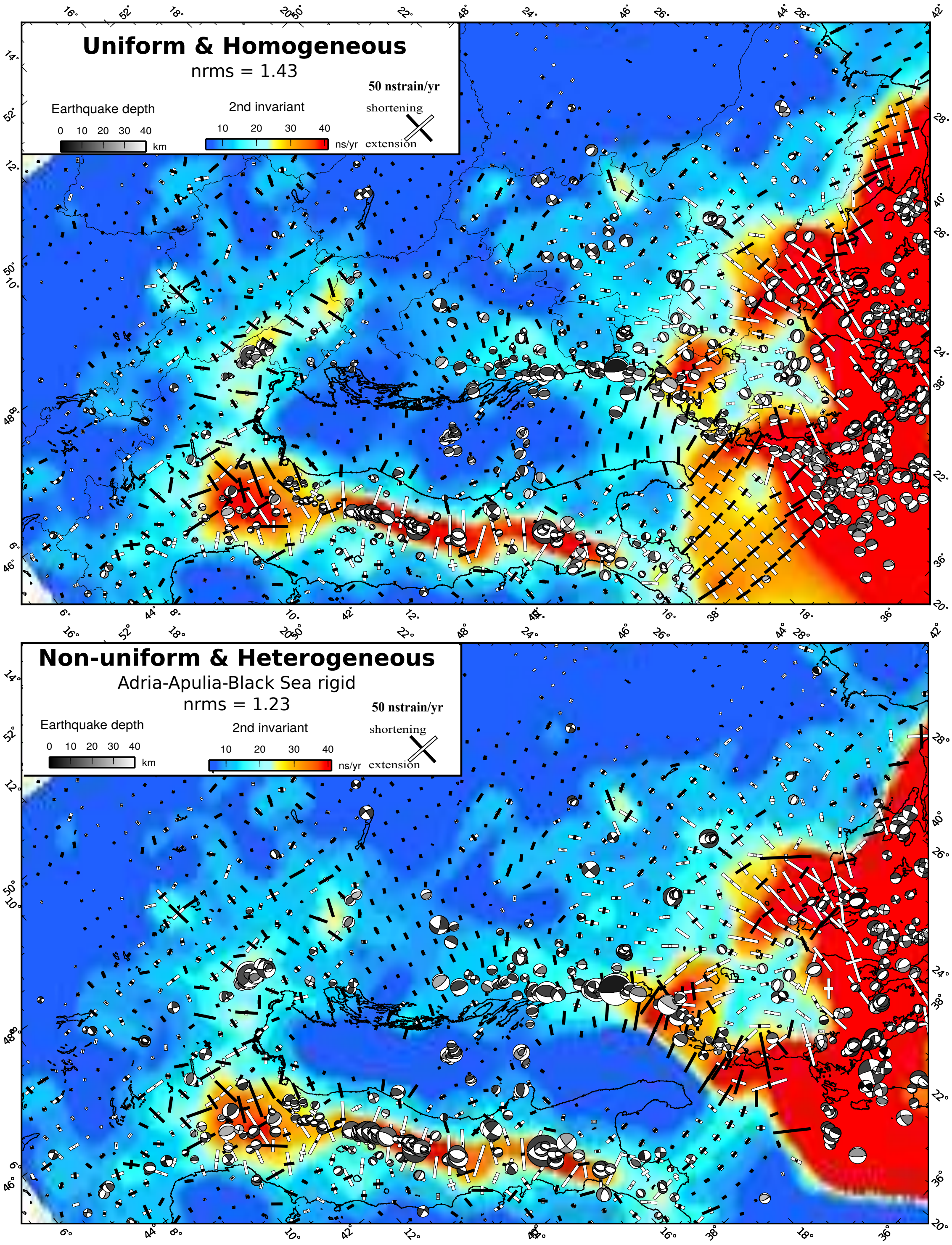

Figure S7. Second invariant of the strain tensor and principal strains direction for an **homogeneous uniform** (A) and **non-uniform non-homogeneous** (B) inversions of the observed velocity field. The non-uniform non-homogeneous model allows for higher strain rates in the NAF and Hellenic backstop (1 and 2 blue in Fig.S4) and Apulia, Adria and Black sea are forced to be rigid (2, 3 and 4 red in Fig.S4); while the homogeneous uniform model does not include constrains from focal mechanisms on the strain direction and allows the same strain rate for all cells. The normalized root mean square in the Balkan area are indicated.

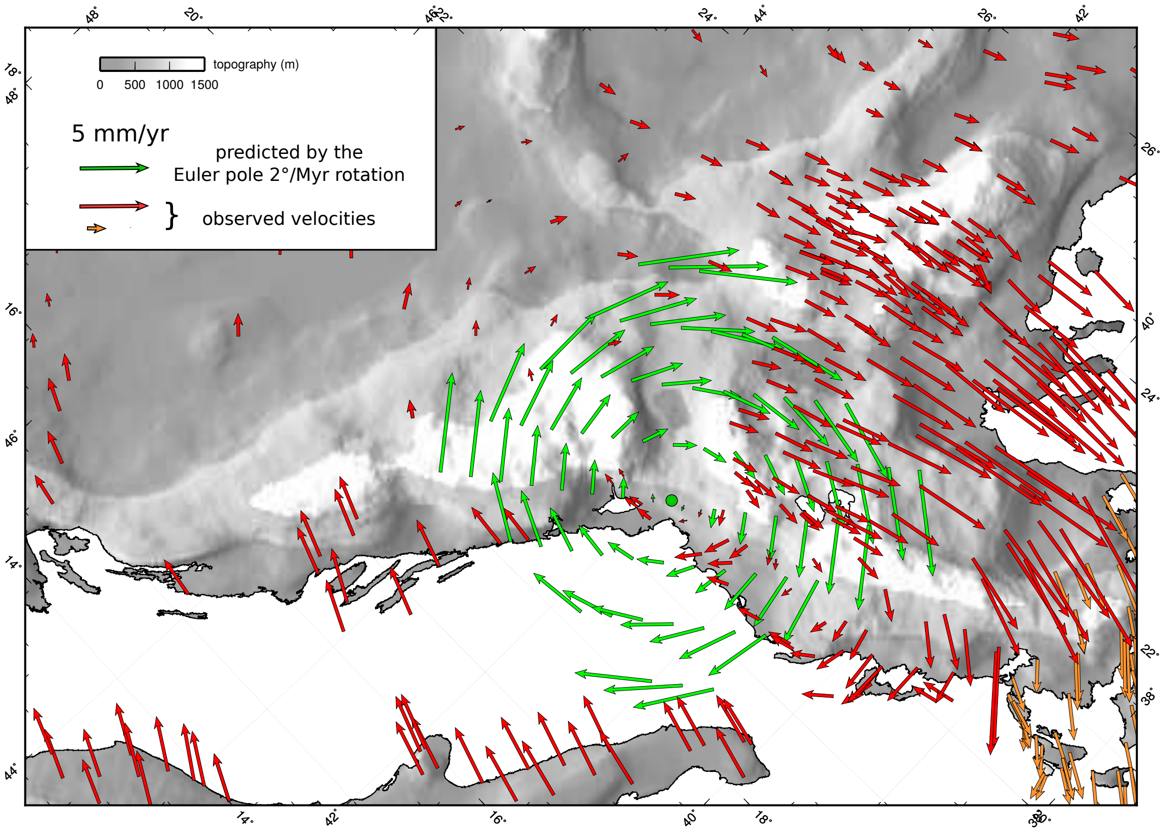

Figure S8. Comparison between observed (red and orange arrows) velocities and the velocities predicted (green arrows) by a (2°/Myr) rotation around a Euler pole located in the Scutari-Peck area (green dot) as suggested by *Kissel et al.* [1995] from paleomagnetic measurements.

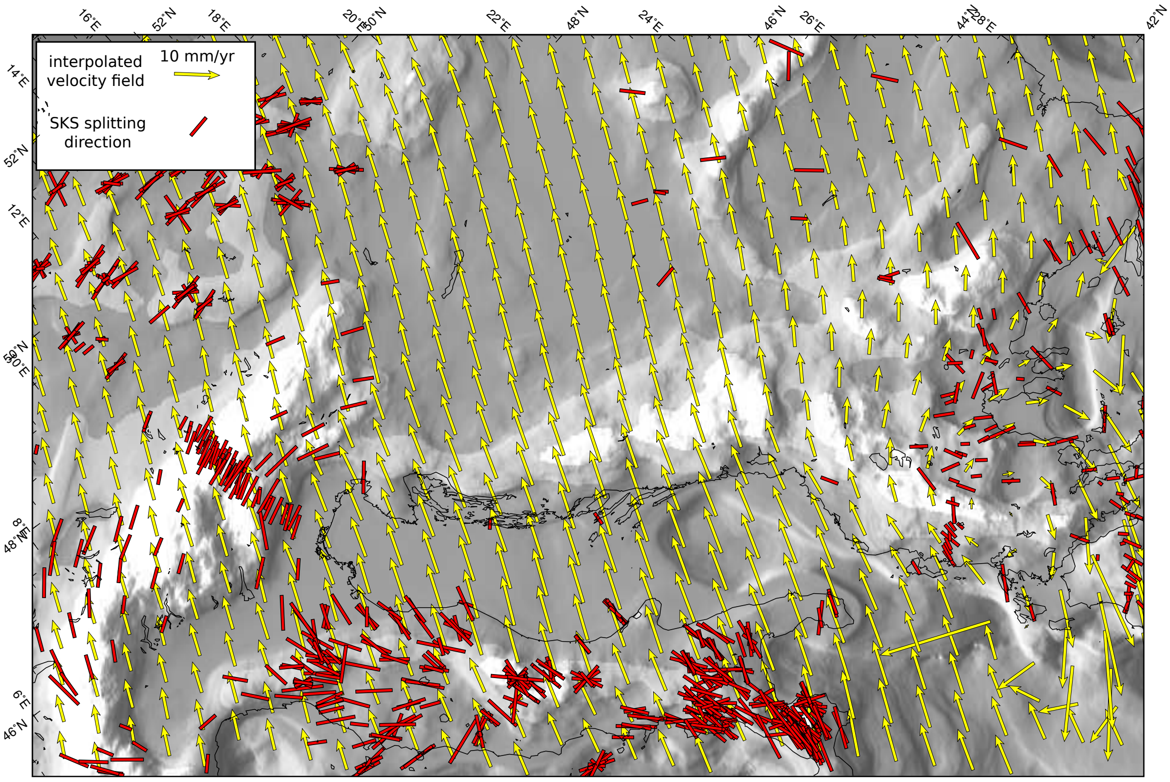

Figure S9. SKS splitting fast axis (red bars) from *Wüstefeld et al.* [2009] and the SKS data base. The length of the bar is proportional to the delay δt but scale is arbitrary. Yellow arrows stand for the interpolated velocity field from our best model plotted in the GRSM-Absolute Plate Motion reference frame from [*Kreemer*, 2009].

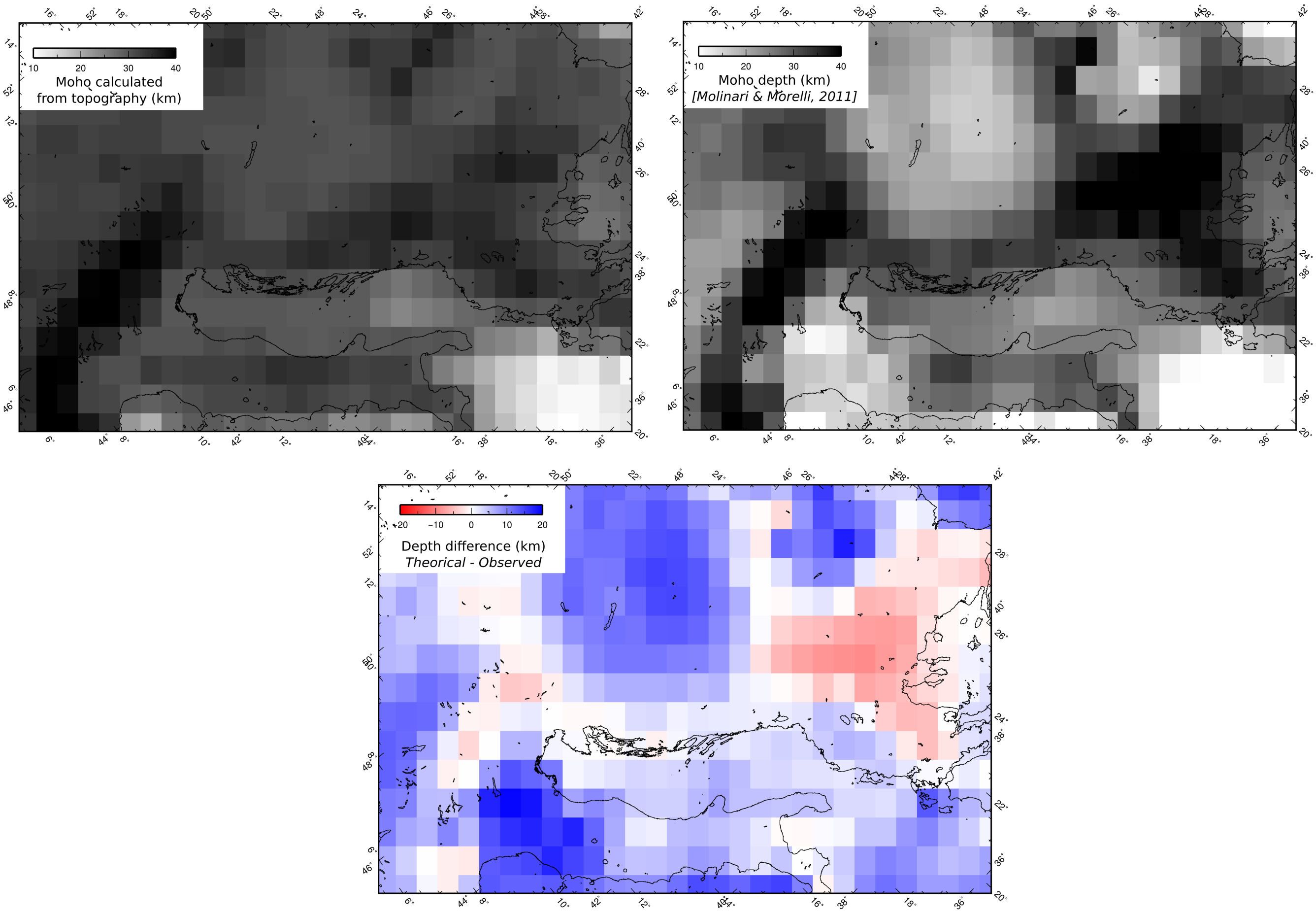

Figure S10. Top left : Moho depth calculated from topography assuming Airy isostasy relative to a reference no relief column of lithosphere for which the crust is 30 km width. The reference level is chosen to be 100 km, ρ_c and ρ_m are chosen to be 2800 and 3300 kg.m^{-3}, respectively. Top right : Moho depth derived from the EPCrust model from *Molinari and Morelli* [2011]. Bottom : discrepancy (in km) between both Moho depth.

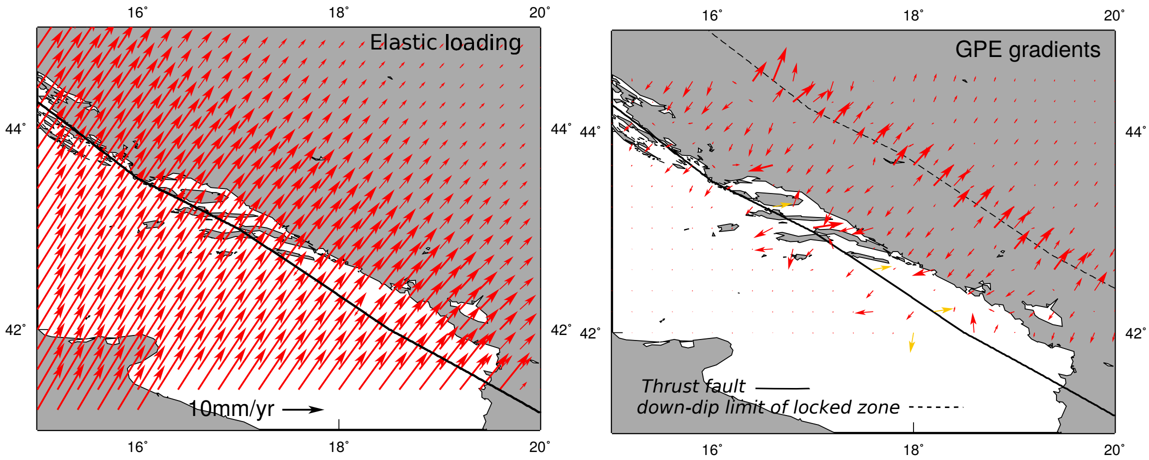

Figure S11. Synthetic test presenting the signature of an interseismically locked thrust front on the surface velocity field (left) and the calculated GPE* (right). Here we chose to lock the 15° dipping Dinarides eastern thrust front down to 30 km depth. This calculation has been conducted using the Defnode code based on the Okada formalism [*McCaffrey*, 2005].

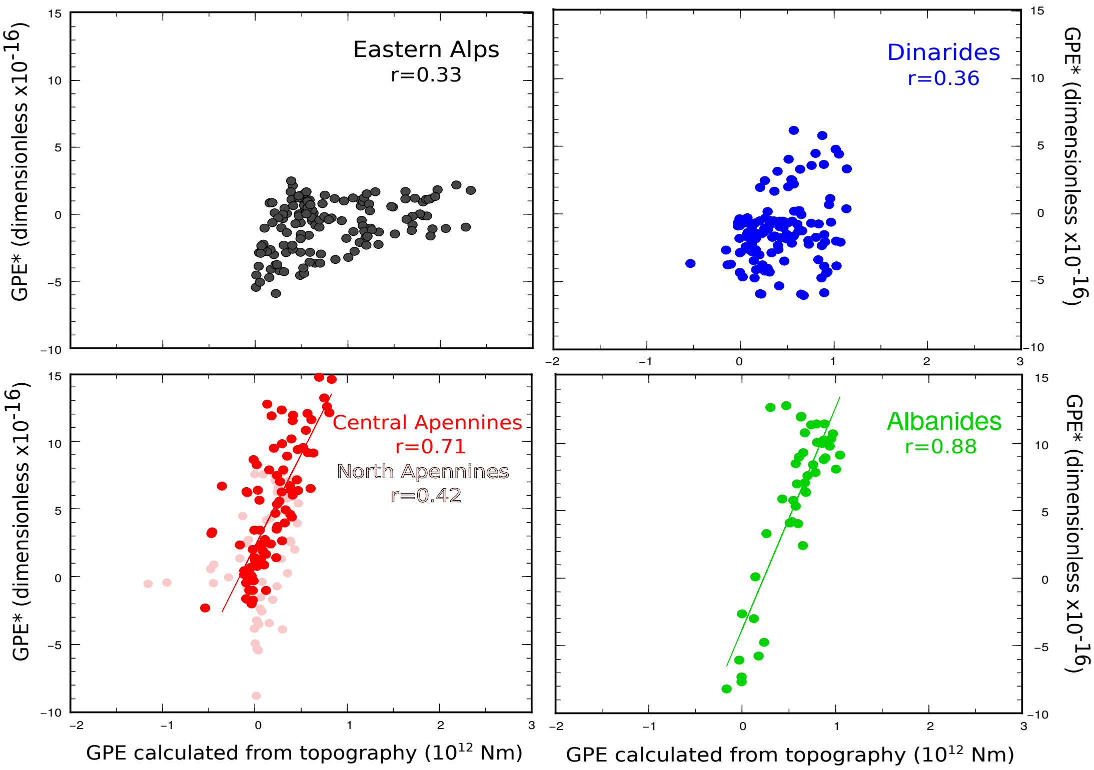

Figure S12. Same than Figure 8 but for a newtonian lithosphere's rheology.

Network	Description	Website
ABRUZZO	Regional network Abruzzo	http://gpsnet.regione.abruzzo.it
ASI	Italian Space Agency	ftp://geodaf.mt.asi.it
CALABRIA	Regional network Calabria	http://gpscalabria.protezionecivilecalabria.it
CISAS	Regional network Veneto	http://147.162.229.63/Web/index.php
EMILIA	Regional network Emilia	http://www.gpsemiliaromagna.it
EUREF	European Reference Frame	http://www.epncb.oma.be
FREDNET	Friuli Regional Deformation Network	www.crs.inogs.it
FVG	Regional network Friuli-Venezia	http://gps.regione.fvg.it
GREF	Geodetic Reference Network of Germany	ftp.igs.ifag.de
IGS	International GNSS Service	ftp.igs.ensg.ign.fr
ISPRA	Istituto Superiore per la Protezione e la Ricerca Ambientale	http://www.isprambiente.gov.it
ITALPOS	Leica Italian Network	http://smartnet.leica-geosystems.it
UMBRIA	GPS Network University of Perugia	http://labtopo.ing.unipg.it
LIGURIA	Regional Network Liguria	www.gnssliguria.it
PIEMONTE	Regional Network Piemonte	http://gnss.regione.piemonte.it
PUGLIA	Regional Network Puglia	http://gps.sit.puglia.it
RGP	Spanish National Network	rgpdata.ign.fr
RING	Italian National Network	http://ring.gm.ingv.it
SONEL	French Oceanographic Network	http://www.sonel.org/-GPS-.html
STPOS	South Tyrolean Positioning Service	www.provincia.bz.it
UNAVCO	University NAVSTAR Consortium	www.unavco.org/data/data.html

Table S3. Description and address of the Networks processed for the large Eastern Mediterranean area.